GEOLOGINEN TUTKIMUSLAITOS

BULLETIN
DE LA
COMMISSION GÉOLOGIQUE
DE FINLANDE
N:o 208

THE CRYSTAL STRUCTURE OF STOKESITE, $CaSnSi_3O_9 \cdot 2H_2O$

BY
ATSO VORMA

WITH 14 FIGURES AND 15 TABLES IN TEXT

HELSINKI 1963

GEOLOGINEN TUTKIMUSLAITOS
BULLETIN DE LA COMMISSION GÉOLOGIQUE DE FINLANDE N:o 208

THE CRYSTAL STRUCTURE OF STOKESITE, $CaSnSi_3O_9 \cdot 2H_2O$

BY
ATSO VORMA

WITH 14 FIGURES AND 15 TABLES IN TEXT

HELSINKI 1963

Helsinki 1963. Valtioneuvoston kirjapaino

ABSTRACT

The structure of stokesite, $4(CaSnSi_3O_9 \cdot 2H_2O)$, has been determined by two-dimensional Fourier methods. The space group is *Pnna* and the unit cell dimensions are: $a = 14.465 \pm 0.005$ Å, $b = 11.625 \pm 0.004$ Å, and $c = 5.235 \pm 0.003$ Å. Spiral-like chains of composition $(SiO_3)_n$ run parallel to the b axis. The repeat unit in the tetrahedral structure is six tetrahedra. Thus the structure of stokesite represents a new kind of chain silicate. The chains are bound together by octahedrally coordinated Sn^{4+} and also octahedrally coordinated Ca^{2+} ions. The coordination octahedron $[SnO_6]$ is almost regular, the average Sn—O distance being 2.033 Å. The coordination polyhedron $[CaO_6]$ is more irregular. The average Ca—O distance is 2.376 Å.

In addition to the crystal structure determination the indexed powder data table is given. The elimination of many coincident reflections from this table is based on the theoretical intensity calculations.

PREFACE

During the period 1961—1962 I had the opportunity to do x-ray crystallographical work at the Department of Mineralogy and Petrology of the University of Cambridge, England. For this opportunity, I am greatly indebted to Professors W. A. Deer, C. E. Tilley, P. Eskola, and V. Marmo.

This paper gives the results of the research work on the crystal structure of stokesite. This work was the major subject on which I concentrated while staying in Cambridge.

It is a great pleasure to thank Dr. P. Gay under whose supervision this work was done. He also supplied the material used during the investigation. Dr. Gay has offered many helpful suggestions and criticized the manuscript. I should also like to thank him and Dr. C. H. Kelsey for correcting the English of this paper. Dr. Kelsey has in addition given me advice during the work, especially in mathematical problems, and critically read the manuscript.

My thanks are also due to the other members of the staff of the Department of Mineralogy and Petrology for valuable suggestions and discussions. Especially I would like to thank Dr. M. G. Bown and Mr. K. O. Rickson. Dr. M. V. Wilkes kindly gave permission to have the calculations performed on the EDSAC II computer in the Mathematical Laboratory of the University of Cambridge. The programs for these calculations were devised by Mr. M. Wells.

Among the persons to whom I want to express my sincere thanks I will mention Professor K. J. Neuvonen who originally awakened my interest in x-ray mineralogy and crystallography and who has shown great interest in this work. I wish to express my appreciation also for his valuable criticism.

The impetus for this work to be published in this form was provided by my teacher, Professor M. Saksela, to whom this project is of great interest. It is a great pleasure to acknowledge this.

To the director of the Geological Survey of Finland, Professor V. Marmo, I am greatly indebted for encouraging me to specialize in this field of science. He also gave permission to have this work published in the series of the Geological Survey. To my chief, Professor A. Simonen, I am extremely

grateful for his interest and sympathetic attitude without which this work could not have been carried out.

Mrs. Toini Mikkola, Mag. Phil., has kindly helped me with the difficulties of the English language and Mrs. Elsa Järvimäki has drawn the pictures and electron density maps for which I wish to express my appreciation.

This work has been financially supported by the foundation Tekniikan Edistämissäätiö, Helsinki, for which I am very grateful.

Helsinki, January 1963

Atso Vorma

CONTENTS

SUMMARY OF PREVIOUS WORK

Until now stokesite has been examined only twice: 1900 when Hutchinson described it for the first time — preliminary communication was given previously in 1899 (Phil. Mag., ser. 5, vol. 48, p. 480) — and 1960 when Gay and Rickson confirmed its chemical composition, determined the space group, and cell size and gave the x-ray powder data. These data have, in addition, once been used for the identification of the only other known stokesite occurrence in the world (Čech 1961).

The original locality for the material described by Hutchinson, and Gay and Rickson is Roscommon Cliff, St. Just, Cornwall, England, where stokesite occurs in association with axinite. The same material has been used in this work. The other known occurrence of stokesite is in Czechoslovakia in a lithium-bearing pegmatite at Ctidružice near Moravské Budějovice in Western Moravia in association with cryptocrystalline cassiterite.

Hutchinson gave an accurate morphological description of the mineral and showed it to belong to the orthorhombic holosymmetric class with

Table 1. Chemical composition and physical data of stokesite.

	1	2	Physical data
SiO_2	43.1 wt.%		Colourless, transparent
SnO	33.3	33.7 wt.%	Lustre vitreous
CaO	13.45	13.3	$\alpha \parallel c = 1.609$
H_2O	8.6		$\beta \parallel a = 1.6125$
	98.6		$\gamma \parallel b = 1.619$
			$2V_\gamma = 69.5°$ (Na-light)
			Dominant forms {110} and {211}
			Cleavage {101} perfect,
			{100} less perfect
			Fracture conchoidal, brittle
			Hardness about 6, specific gravity 3.185

1. Hutchinson 1900.
2. Gay and Rickson 1960.

Note: The physical data are in accordance with the unit cell determined by Gay and Rickson.

$a : b : c = 0.3463 : 1 : 0.8033$. His microchemical analysis is recorded in Table 1. It leads to the empirical formula $CaSnSi_3O_{11}H_4$. Mention should also be made of the results of Hutchinson's determinations of the water expelled at different temperatures. The mineral remained unchanged at 100°C, heated to 220°C it lost 1.9 per cent, at 350°C the loss amounted to 6 per cent, and the rest of water was given off between 350°C and dull redness. From these numbers Hutchinson concluded that the water is not present as water of crystallization but is bound water.

Gay and Rickson (*op. cit.*) showed by x-ray methods that stokesite is really orthorhombic having the following cell size: $a = 14.41$ Å, $b = 11.61$ Å, and $c = 5.23$ Å (all ± 0.03 Å). The space group was shown to be *Pnna*. They also confirmed the CaO and SnO content of the mineral by x-ray emission micro-analytical technique (Table 1) and showed the unit cell content to be 4 ($CaSnSi_3O_{11}H_4$). The cell used by Gay and Rickson is derived from Hutchinson's morphological unit by the transformation 010/001/100.

Physical properties given by Hutchinson and recorded by Gay and Rickson are also repeated here because they are dependent on the crystal structure (Table 1).

UNIT CELL SIZE DETERMINATION AND THE POWDER DATA

During the refinement of the structure the lengths of the a, b, and c axes given by Gay and Rickson (1960) were used. At the end of the accuracy estimation it became clear that the inaccuracy in the unit cell size was one of the greatest sources of error in the interatomic distances. Therefore it seemed reasonable to redetermine the cell size more accurately so that the remaining possible errors would have no influence upon the final interatomic lengths and angles.

For this purpose the Unicam back reflection flat plate camera was used with silicon as internal standard (crystal to film distance being about 25.3 mm varying slightly for different films). Cu-radiation was used and the results shown in Table 2 were obtained. Using such derived values for cell dimensions it is possible to discount the influence of inaccuracy in cell size upon the interatomic lengths and angles.

An attempt was also made to determine the unit cell size from the powder data. This was unsuccessful because the high angle reflections overlapped. The theoretical intensities of all reflections inside the limiting sphere for CuKα-radiation were calculated and compared with the observed powder

Table 2. The data for unit cell size determination.

Reflection	Radiation	Cell dimensions
18.0.0	CuKα_1	$a = 14.466$ Å
	CuKα_2	$a = 14.463$ Å
0.16.0	CuKβ_1	$b = 11.625$ Å
0.15.1	CuKβ_1	$b = 11.626$ Å
		(supposing $c = 5.235$ Å)
006	CuKα_1	$c = 5.2350$ Å
	CuKα_2	$c = 5.2351$ Å
		Mean $a = 14.465 \pm 0.005$ Å
		$b = 11.625 \pm 0.004$ Å
		$c = 5.235 \pm 0.003$ Å

Note: The accuracy estimated from the formula $\Delta d = d \cdot tg\Phi\Delta\Phi$

Table 3. Indexed powder data for stokesite. Measurements by Gay and Rickson 1960, indexing and d_c by Vorma.

hkl	*I*	d_o	d_c	*hkl*	*I*	d_o	d_c
200	s	7.25	7.232	442			1.713
020	m	5.82	5.812	551	m	1.711	1.712
101	vw	4.95	4.922	460			1.708
011	w	4.79	4.773	622	vw	1.694	1.696
220	m	4.54	4.531	213	m	1.678	1.678
211	vs	3.99	3.984	651	w	1.593	1.594
121	w	3.76	3.756	062			1.557
301	m	3.55	3.546	413	ms	1.556	1.557
221	m	3.43	3.426	233			1.554
321	m	3.03	3.027	271	vw	1.545	1.546
040			2.906	840	vw	1.534	1.535
411	vs(b)	2.89	2.883	262	vw	1.521	1.522
231			2.861	642	m	1.511	1.513
240	m	2.69	2.697	660			1.510
421	vw	2.65	2.648	802	m	1.486	1.487
430			2.644	433			1.456
002	w	2.62	2.618	080	w(b)	1.451	1.453
501	vw	2.52	2.532	471			1.450
511	vw	2.47	2.466	822	vw	1.440	1.440
022	m	2.39	2.386	462			1.431
431	vw	2.36	2.360	343	w(b)	1.427	1.429
122			2.355	280			1.425
222	m	2.27	2.267	10.1.1	m	1.384	1.384
440			2.265	253	vvw	1.370	1.370
620	m	2.23	2.227	842			1.324
611	m	2.15	2.152	671	m	1.322	1.323
051	m	2.12	2.125	860			1.322
402			2.120	10.3.1	w	1.309	1.312
630	m	2.04	2.047	004			1.309
251			2.039	453	w	1.302	1.302
422	vw	1.992	1.992	091			1.254
042	w	1.938	1.945	363	vw	1.253	1.252
631	w	1.906	1.906	282			1.248
242	vw	1.877	1.878	291	vw	1.235	1.235
451	m	1.832	1.832	10.5.1	vvw(b)	1.194	1.196
800	w	1.808	1.808	044			1.194
602	m	1.774	1.773	862	vvw(b)	1.178	1.180
612	vw	1.755	1.753	244			1.177
820	w	1.726	1.726	473	vw	1.141	1.141
				624	w	1.128	1.128
				682	w	1.125	1.124

lines. The indices of many planes could be eliminated because the calculated intensity of the reflections from these planes is weak. However, so many remained that it was impossible to index unambiguously all the powder lines given in the table published by Gay and Rickson. No additional lines have been listed in Table 3 which gives the measured d-spacings of Gay and Rickson and the corresponding indices deduced using the theoretical intensity data. The spacings of the planes have been recalculated using the new unit cell size.

INTENSITY DATA

COLLECTION OF THE DATA

The intensity data were collected by triple-film Weissenberg patterns using Mo-radiation and Zr filter. The reflections from *hk*0-, 0*kl*-, and *h*0*l*-layer lines were recorded. The films were interleaved with thin tin foil which reduced the intensity by approximately 1/2. They were exposed for about 30 days, 5 days, 16 hours, and some few hours respectively. The intensities were estimated visually by comparison with an intensity scale, prepared in the Weissenberg camera by selecting the 060 reflection and oscillating it n, 2n, 3n, . . . 15n times through the reflecting position. When measuring the intensities of reflections where the $\alpha_1\alpha_2$ doublets were only partially resolved linear interpolation was used to estimate the combined effect. Where $\alpha_1\alpha_2$ doublets were completely resolved their sum was accepted as peak intensity. When a collimator with an aperture of 0.5 mm was used it is likely that the plateau in the centre of the spot is achieved and the peak intensity actually represents the integrated intensity (Buerger 1960, p. 84).

Intensity data were collected in all three projections to the value of $\frac{\sin\Theta}{\lambda} = 1.35$ Å^{-1}. For the (001)-projection as a whole 314 independent *hk*0 reflections were recorded, for the (100)-projection the corresponding figure was 173 and for the (010)-projection it was 145. The intensity data for each projection, read from various films, were placed on the same relative scale by using appropriate film factors based on the comparison of intensity readings of reflections recorded on more than one film.

Due to the small size of the stokesite crystal used in these measurements it was not possible to record very weak reflections even though the longest exposure times were as long as 30 days. The used technique gave a range of scaled intensities of approximately 1 to 750.

During the early stages of the refinement the data for each projection have been treated independently. In the stage when the scaling seemed to

be accurate enough the mean was taken from each axial reflection occurring in more than one projection and these values were used during the latter stages.

CORRECTIONS TO THE DATA

All the recorded intensities were corrected for Lorenz-polarization factors using the charts of Cochran (1948).

The linear absorption coefficient μ for stokesite was calculated using the unit cell content and cell size given by Gay and Rickson (1960) and specific gravity given by Hutchinson (1900). For molybdenum radiation it turned out to be 41.9 cm^{-1}. The optimum thickness of stokesite crystal for oscillation photographs would thus be $2/\mu = 0.49$ mm (Buerger 1949, pp. 179—181). The size of the used stokesite crystal was about 0.2 mm (almost equi-dimensional fragment). Supposing that the crystal is a sphere with a radius of 0.1 mm, the transmission factor for MoKα-radiation would vary from 0.546 to 0.570 when Θ varies from 0° to 90° (Evans and Ekstein 1952). The corresponding corrections to the structure factors are so small that they have been omitted. Nevertheless it is certain that there is an absorption effect for the strongest low angle reflections, especially since the crystal used is not a sphere.

Partial allowance for secondary extinction has been made by omitting the most intense low angle reflections from the (F_o—F_c)-syntheses during the refinement. However, almost all the F_o have been included in difference maps presented, F_{200} and F_{040} being the only exceptions. In the final F_o-syntheses only these two have been replaced by the corresponding F_c. As a result of this the final difference maps show some features which indicate small shifts for some atoms and also adjustments of some temperature parameters. Remembering that these features are at least partly due to extinction and probably also to absorption it was thought that these small adjustments are not well founded. The magnitude of these features on the difference maps is small compared to the absolute value of the electron density at these positions on the final electron density maps showing that extinction and absorption errors are amall.

OTHER CONSIDERATIONS

All two-dimensional Fourier syntheses and greatest part of the structure factor calculations were carried out on the EDSAC II computer in the Mathematical Laboratory of the University of Cambridge, England. The programs were devised by Mr. M. Wells.

For the atomic scattering curves the analytical approximation $f(x) = Ae^{-ax^2} + Be^{-bx^2} + C$ was used with the constants as follows (Forsyth and Wells 1959):

	A	a	B	b	C
O	2.113	2.867	4.637	14.75	1.211
Sn	22.32	1.722	16.06	17.93	10.98
Ca^{2+}	7.062	0.8174	8.893	11.63	2.017
Si^{4+}	5.138	1.459	3.442	3.982	1.420

At the end of refinement it seemed more obvious that the Sn atom was in an ionized state. The average Sn—O distance in the $[SnO_6]$ coordination group turned out to be 2.033 Å indicating Sn^{4+} ion (see p. 43). The structure factor calculations were performed using the atomic scattering curve for neutral Sn atom. On account of this an approximate atomic scattering curve was drawn for Sn^{4+} ion and corresponding corrections were performed to the very low angle reflections. The corrections were as a whole very small and had very little influence on the final reliability index R. Similar estimations were made to allow for the differences between the scattering curves of O and O^{2-}. In this structure the influence of the possible ionization of oxygen atoms turned out to be so small that no corrections were made to the calculated structure factors.

During the calculations of the projections on (001) of the Patterson function and electron density maps the halved value of the a axis was used and the origin was taken at a different position to that in the three dimensional space group. In the data given here the origin is always that of the three-dimensional space group $Pnna$ ($\bar{1}$) and the sampling of points along the x direction always refers to the 14.465 Å-axis. The signs of the structure

factors have also been altered to correspond to the common origin, and the indices of the reflections are given in accordance with the three-dimensional space group and not with the two-dimensional plane group (*pgm*; $a' = a/2$, $b' = b$), where the h index is always halved. In the projections on (010) and (100) the length of the axes is the same as in three-dimensional unit cell, but the origin of the former projection is in a different position to that in the space group *Pnna*. The published data for this projection are also referred to the conventional unit cell of the space group *Pnna*.

The theoretical structure factors have been calculated for two formula units of stokesite ($2CaSnSi_3O_{11}H_4$). The structure factors for the whole unit cell are thus twice those given in this work. As is to be expected in this kind of structure the influence of hydrogen atoms upon the structure factors is small and therefore has been omitted.

All the coordinates of atoms in this paper are referred to the three-dimensional unit cell.

DEDUCTION OF THE TRIAL STRUCTURE

Hutchinson (1900) suggested the formal resemblance of stokesite to catapleiite ($Na_2ZrSi_3O_{11}H_4$). Gay and Rickson (1960) showed that the powder photographs of these two minerals show very little resemblance. Catapleiite contains three membered $(SiO_3)_3$ rings. However, before the intensity data for stokesite were available, a trial structure with a three membered ring was deduced. Subsequent structure factor calculations and F_o-synthesis using 70 independent reflections showed this model to be wrong. Only the tin atom was later shown to be in the correct place.

Gay and Rickson suggested, referring to the length of the c axis (5.23 Å), that the Si—O tetrahedral arrangement is more closely related to those of the normal band or sheet silicate structures than to that of the ring model.

Stokesite has the space group *Pnna* and accordingly the number of general equivalent positions in a unit cell is eight. Since there are four Sn, four Ca, twelve Si, and 44 O atoms in a unit cell, it is clear that Sn, Ca, at least four Si and four O atoms occupy special equivalent positions (in this space group there are four sets of special equivalent positions). Looking at Weissenberg photographs of different layer lines shows that the reflections with h and $k + l$ even are the most intense in the back reflection area. The heavy atom tin must be the main contributor to strong high angle reflections, and thus the tin atom must be located on one of the two sets of special equivalent positions on the centres of symmetry (Positions 4*a* and 4*b* in the Wyckoff notation: International Tables for X-ray Crystallography, Vol. I, p. 140, 1952). In addition the tin atom could be located in the special position 4*c* on the diad parallel to the c axis. If the z coordinate is either 0 or ½ (in fractional coordinates) then the reflections with h and $k + l$ even would be very strong compared with the other reflections. Thus it is possible to locate the Sn atom on 4*a*, 4*b*, or 4*c*, the two first mentioned being sets of symmetry centres and the last one being a set of equipoints on the diads parallel to the c axis.

Using further the symmetry elements of this space group it is possible to conclude that at least four of the twelve Si atoms in the unit cell must be located on a diad (4*c* or 4*d*) since an $[SiO_4]$ tetrahedron is not centrosym-

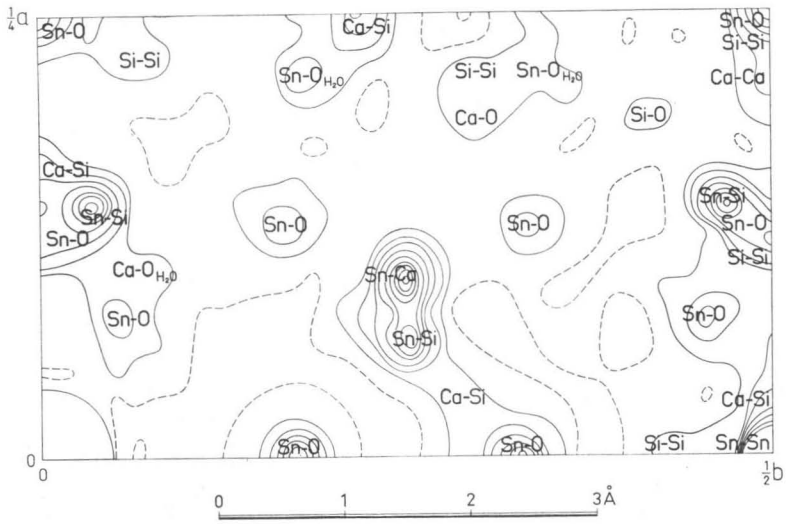

Fig. 1. Projection of the Patterson function of stokesite on (001). Contours at equal arbitrary intervals. The broken lines indicate negative contours.

metric. Attempts to derive a trial structure, based on the known silicate linkages, from packing considerations were unsuccessful.

When it turned to be impossible to deduce the trial structure by the methods described above, the projection of the Patterson function of stokesite on (001) was calculated using about 300 independent $|F_o|^2$. The sampling interval along each axis was 1/128. Fig. 1 shows the asymmetric part of the projection of the Patterson function. This part is repeated by symmetry (*pmm*) to cover the whole projection of the unit cell. The origin peak has been omitted from the map as well as the centre of the peak indicating the Sn—Sn vector. From this vector map it was possible to deduce a trial structure which at first was not quite convincing due to the very strange $(SiO_3)_n$ chain framework. However, it later on refined very well.

The positions of the more important interatomic vectors are indicated on the vector map. The coordinates of atoms deduced from this map are listed in Table 4. When comparing these figures with the final coordinates (Table 5) it is seen that the most noticeable difference is in the coordinates of O_I, which was believed to coincide in the (001)-projection with the Si_{II} atom. z coordinates were determined at this stage by means of packing considerations. Sn atoms occupy the symmetry centre 4*b* according to this interpretation, and Ca and Si_I atoms are located on diads parallel to the a axis (4*d*). Four oxygen atoms are situated on diads parallel to the c axis (at 4*c*) and the rest of the Si and O atoms occupy general positions in the unit cell.

Table 4. The coordinates of atoms in the unit cell of stokesite derived from (001)*-Patterson projection.*

Atom	Position (Wyckoff notation)	x	y	z
Sn	4 *b*	0	0	½
Ca	4 *d*	.398	¼	¼
Si_I	4 *d*	.064	¼	¼
Si_{II}	8 *e*	.142	.032	.00
O_I	8 *e*	.140	.035	.60
O_{II}	8 *e*	.130	.168	.05
O_{III}	8 *e*	.423	.047	.20
O_{IV}	8 *e*	.000	.172	.45
O_{H_2O}	8 *e*	.285	.177	.55
O_V	4 *c*	¼	0	.10

Note 1: z coordinates have been deduced on the basis of packing of atoms in the unit cell.

Note 2: The locations of atoms in every set 4*b*, 4*c*, 4*d*, and 8*e* are given in Table 5.

At this stage structure factors were calculated for the strongest reflections using the coordinates of the atoms in the trial structure. The R factor for approximately 70 $hk0$ reflections was about 25 %. An approximate scaling factor was used. No temperature factor was included.

REFINEMENT OF THE STRUCTURE

The refinement of the structure was based on F_o-syntheses and several cycles of difference syntheses on every projection. The projections used were (001), (010), and (100). Fig. 2 shows the relations of the two-dimensional plane groups of the projections to the three-dimensional space group (*Pnna*). The space group *Pnna* projects along [001] as *p2gm* and along [010] and [100] as *c2mm*. In the (001)-projection the a' axis is half the original a axis (in *Pnna*). Other axes and also the a' axis in the other projections remain unchanged. In Fig. 2 the shaded area represents the asymmetric unit used in each projection. The cell edges a and b were sampled at 128, the cell edge c at 64 uniformly spaced points. x and y coordinates were determined from the projection on (001) while the z coordinate was deduced from the other two projections.

REFINEMENT OF THE PROJECTION ON (001)

The projection on (001) was refined calculating first the F_o-synthesis using only some 140 independent reflections. The artificial termination of the Fourier series produces diffraction ripples around each atom and accordingly the apparent coordinates of every atom are slightly shifted. Because series termination effects are especially noticeable about heavy atoms, all the electron density syntheses of stokesite showed a series of negative and positive rings around the Sn peak. In the early stages of refinement these ripples were so strong that for example the atom O_I was not resolved at all and was therefore thought to coincide with Si_{II}. At this stage, however, it was evident that the structure deduced from the Patterson function was correct.

For this projection 314 independent F_{hk0} were measured, of which 66 were those for which k is odd and 248 for which k is even. The first mentioned 66 reflections are those on which tin has no influence whereas the other reflections with k even are affected by tin. This uneven distribution of reflections produces some »ghost» features in the corresponding electron

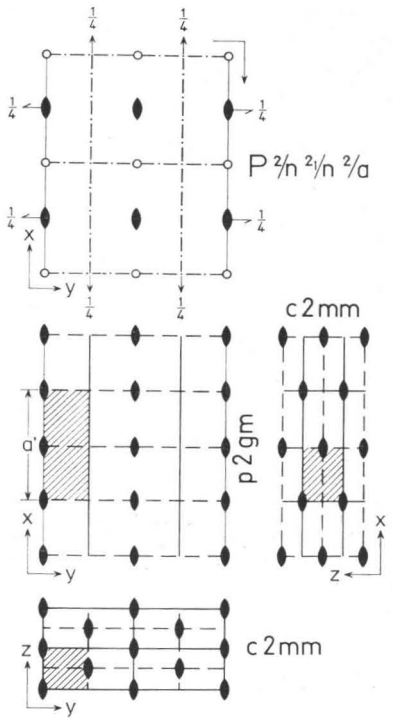

Fig. 2. Schematical representation of the relations between the three-dimensional space group *Pnna* and the axial projections of it. The shaded area in each two-dimensional projection represents the asymmetric unit used in the electron density and difference maps.

density map. There is a marked tendency for the b axis to be halved and the corresponding two parts of the projection superposed. Two cycles of difference syntheses were performed. Scaling was only approximate and no temperature factor was yet used. Wilson's statistical method of determining the temperature factor (Wilson 1942) was tried but did not give a reliable value. At this stage the structure was refined to the stage that the signs for almost all observed reflections were determined. A new F_o-synthesis was calculated using 305 independent reflections. O_I was now clearly resolved. At the same time a partial Fourier synthesis was calculated using only the reflections for which the k index was odd. This synthesis clearly interpreted the negative areas around each ghost peak (Fig. 4) on the electron density map. The result corresponds to the situation of adding two Fourier series

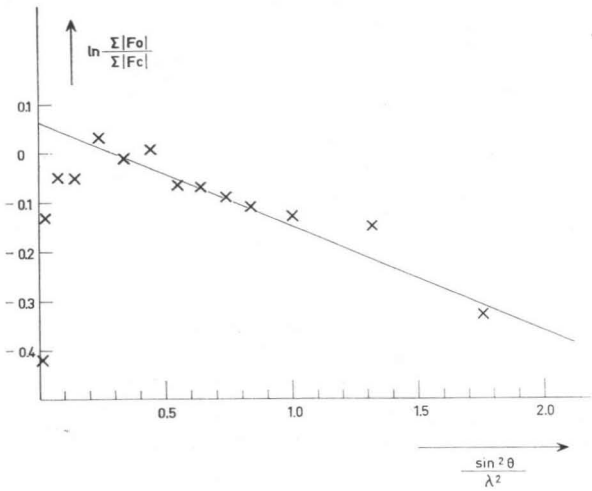

Fig. 3. Graph for finding the temperature parameter B and the scaling factor for stokesite in (001)-projection. Note the influence of absorption and extinction.

together of which one is terminated at small value of $\frac{\sin \Theta}{\lambda}$ and the other corresponding to a halved y axis at a high value. The atomic peaks in the first are broad, in the other sharp. Both of these series show maxima at the positions of actual atoms and the electron density is the sum of these series at the corresponding point. If the two series were terminated at the same $\frac{\sin \Theta}{\lambda}$ value, the sum at the positions of ghost peaks would be zero and this disturbing effect thus avoided.

A further set of F_c were calculated and values for the isotropic temperature factor B and the scaling factor were found using the formula $ln \frac{\Sigma |F_o|}{\Sigma |F_c|} = - \frac{B \sin^2 \Theta}{\lambda^2}$ where $\Sigma |F|$ represents the sum of $|F|$ over a small range of $\left(\frac{\sin \Theta}{\lambda}\right)^2$. If $ln \frac{\Sigma |F_o|}{\Sigma |F_c|}$ is plotted against $\left(\frac{\sin \Theta}{\lambda}\right)^2$ then the slope of the resulting straight line gives a value for B (Fig. 3).

In the (001)-projection this overall temperature factor turned out to be 0.21. Fig. 3 also displays that the low-Θ reflections are affected either by absorption or extinction or both. In subsequent cycles of refinement (five cycles of difference syntheses) individual isotropic temperature factors were determined by the method of Cochran (1951) and the scaling was checked after every cycle. At the stage when the scaling in every projection was

Table 5. The final coordinates of atoms in the unit cell of stokesite.

Atom	Number of positions and Wyckoff notation	Coordinates		Estimated standard deviations
Sn	4 *b*	0, 0, ½ ½, 0, ½ 0, ½, 0 ½, ½, 0		
Ca	4 *d*	x, ¼, ¼ $\bar{x}$, ¾, ¾ ½ + x, ¼, ¾ ½ − x, ¾, ¼	$x = 0.4000$	$\sigma(x) = \pm 0.00022$
Si_I	4 *d*	—»—	$x = 0.0648$	$\sigma(x) = \pm 0.00022$
Si_{II}	8 *e*	x, y, z ½ − x, $\bar{y}$, z x, ½ − y, ½ − z ½ − x, ½ + y, ½ − z $\bar{x}$, $\bar{y}$, $\bar{z}$ ½ + x, y, $\bar{z}$ $\bar{x}$, ½ + y, ½ + z ½ + x, ½ − y, ½ + z	$x = 0.1415$ $y = 0.0317$ $z = 0.0000$	$\sigma(x) = \pm 0.00027$ $\sigma(y) = \pm 0.00029$ $\sigma(z) = \pm 0.00077$
O_I	8 *e*	—»—	$x = 0.1175$ $y = 0.0090$ $z = 0.7050$	
O_{II}	8 *e*	—»—	$x = 0.1315$ $y = 0.1668$ $z = 0.0810$	
O_{III}	8 *e*	—»—	$x = 0.4235$ $y = 0.0480$ $z = 0.1870$	$\sigma(x) = \pm 0.00070$ $\sigma(y) = \pm 0.00095$ $\sigma(z) = \pm 0.0021$
O_{IV}	8 *e*	—»—	$x = 0.0010$ $y = 0.1720$ $z = 0.4295$	
O_{H_2O}	8 *e*	—»—	$x = 0.2870$ $y = 0.1770$ $z = 0.5220$	
O_V	4 *c*	¼, 0, z ¾, 0, $\bar{z}$ ¾, ½, ½ + z ¼, ½, ½ − z	$z = 0.0480$	$\sigma(z) = \pm 0.0021$

believed to be accurate enough the mean was taken of the axial reflections occurring in more than one projection. During the refinement many strong reflections in the very low-Θ region were omitted because of the supposed extinction and absorption. In the final difference synthesis, however, only

Table 6. Final isotropic temperature parameters.

Atom	(001)-projection	(100)-projection	(010)-projection
Sn	.15	.16	.16
Ca	.55	.55	.60
Si_I	.30	.30	.35
Si_{II}	.25	.30	.30
O_I	.55	.55	.55
O_{II}	.70	.80	.80
O_{III}	.60	.60	.60
O_{IV}	.60	.60	.60
O_V	.70	.70	.70
O_{H_2O}	1.00	1.00	1.00

Note: According to the final difference map on (010) the temperature parameters for Sn, Ca, and Si_I are too small.

F_{200} and F_{040} have been replaced by the calculated values. The same applies to the final electron density synthesis (Fig. 4), which was calculated using all the 314 observed independent reflections.

Table 5 shows the atomic coordinates with their estimated standard deviations. In Table 6 the final isotropic temperature factors for all three projections are presented. In Table 7 the F_{hk0} are recorded. The reliability index for all 314 observed reflections was 9.99 per cent.

The final difference synthesis (Fig. 5) indicates some anisotropic temperature movements for Sn, Si_I, Ca, and possibly for Si_{II}. However, the disturbances in the difference synthesis map are so small compared with the electron density in the middle of the corresponding atoms in the F_o-synthesis that it seemed a waste of time to determine the anisotropic parameters in the case of stokesite, especially when the influence of extinction and absorption was uncorrected.

In the electron density map the most marked features are the very high electron densities in the middle of atoms and the sharpness of atomic peaks. This is due to the termination of the Fourier series at very high $\frac{\sin \Theta}{\lambda}$ value (1.35). The other conspicuous feature is the diffraction rings about the atoms, especially about tin. These rings could have been avoided by using artificial temperature factors. However, the actual refinement was done using difference syntheses where the series termination effects overcome and so there was no need to apply an artificial temperature factor. The third already mentioned feature in the electron density map is the occurrence of ghost peaks. The ghost peaks for Ca, Si_I, Si_{II}, O_{II}, O_{III}, and O_{H_2O} are clearly shown. For Sn and O_V there are no ghost peaks because they do not have any influence of the F_{kh0} with k odd. The ghost peak of O_{IV} almost coincides

Table 7. Observed and calculated hk0-structure factors for stokesite.

h k 0	F_o	F_c	h k 0	F_c	F_o	h k 0	F_o	F_c
0 0 0	—	370	4 9 0	19	15	8 3 0	—	2
0 2 0	88	91	4 10 0	80	79	8 4 0	64	74
0 4 0	133	171	4 11 0	13	10	8 5 0	32	—31
0 6 0	95	114	4 12 0	57	53	8 6 0	90	111
0 8 0	77	76	4 13 0	—	—7	8 7 0	23	—23
0 10 0	—	12	4 14 0	68	63	8 8 0	54	54
0 12 0	77	80	4 15 0	—	0	8 9 0	33	—27
0 14 0	—	—5	4 16 0	48	46	8 10 0	58	60
0 16 0	48	47	4 17 0	—	—8	8 11 0	—	5
0 18 0	26	24	4 18 0	52	52	8 12 0	55	52
0 20 0	41	36	4 19 0	—	—6	8 13 0	22	—19
0 22 0	20	20	4 20 0	28	26	8 14 0	37	37
0 24 0	48	42	4 21 0	—	—3	8 15 0	19	15
0 26 0	—	15	4 22 0	42	38	8 16 0	28	25
0 28 0	34	32	4 23 0	—	—3	8 17 0	—	0
0 30 0	17	19	4 24 0	15	19	8 18 0	39	37
			4 25 0	—	—2	8 19 0	14	11
2 0 0	70	113	4 26 0	25	22	8 20 0	14	18
2 1 0	—	2	4 27 0	—	1	8 21 0	—	3
2 2 0	58	59	4 28 0	18	17	8 22 0	29	26
2 3 0	31	—27	4 29 0	—	—2	8 23 0	—	11
2 4 0	75	87	4 30 0	15	18	8 24 0	28	27
2 5 0	7	6				8 25 0	—	—1
2 6 0	45	39	6 0 0	46	45	8 26 0	27	23
2 7 0	45	—42	6 1 0	19	16	8 27 0	—	7
2 8 0	64	67	6 2 0	72	84	8 28 0	22	23
2 9 0	25	—25	6 3 0	51	45	8 29 0	—	—1
2 10 0	37	30	6 4 0	27	23	8 30 0	26	27
2 11 0	31	—25	6 5 0	20	—15			
2 12 0	63	59	6 6 0	91	105	10 0 0	63	62
2 13 0	20	—18	6 7 0	66	72	10 1 0	—	2
2 14 0	35	32	6 8 0	24	23	10 2 0	19	17
2 15 0	20	—18	6 9 0	—	4	10 3 0	33	—33
2 16 0	53	47	6 10 0	73	66	10 4 0	45	45
2 17 0	—	4	6 11 0	34	26	10 5 0	16	—10
2 18 0	34	32	6 12 0	32	27	10 6 0	46	48
2 19 0	—	—4	6 13 0	11	8	10 7 0	36	—35
2 20 0	40	38	6 14 0	44	42	10 8 0	45	48
2 21 0	—	8	6 15 0	17	12	10 9 0	16	—11
2 22 0	26	23	6 16 0	—	10	10 10 0	52	46
2 23 0	—	7	6 17 0	18	—13	10 11 0	19	—14
2 24 0	36	30	6 18 0	40	37	10 12 0	67	65
2 25 0	—	7	6 19 0	14	11	10 13 0	—	1
2 26 0	14	16	6 20 0	—	7	10 14 0	38	38
2 27 0	—	2	6 21 0	15	—13	10 15 0	—	—8
2 28 0	23	21	6 22 0	36	29	10 16 0	50	53
2 29 0	—	5	6 23 0	—	1	10 17 0	—	10
2 30 0	15	15	6 24 0	14	17	10 18 0	32	37
			6 25 0	—	—5	10 19 0	—	—3
4 0 0	19	16	6 26 0	25	26	10 20 0	35	33
4 1 0	10	—6	6 27 0	—	2	10 21 0	—	3
4 2 0	46	46	6 28 0	22	18	10 22 0	26	26
4 3 0	36	29	6 29 0	—	—4	10 23 0	—	—1
4 4 0	22	15	6 30 0	33	28	10 24 0	28	26
4 5 0	36	32				10 25 0	—	0
4 6 0	73	78	8 0 0	103	119	10 26 0	12	13
4 7 0	20	17	8 1 0	42	—47	10 27 0	—	—4
4 8 0	36	33	8 2 0	74	95	10 28 0	20	19

Table 7. (Continued).

h k 0	F_o	F_c	h k 0	F_o	F_c	h k 0	F_o	F_c
10 29 0	—	2	14 25 0	—	7	18 22 0	25	21
10 30 0	13	12	14 26 0	18	19	18 23 0	—	5
			14 27 0	—	—1	18 24 0	23	22
12 0 0	51	51	14 28 0	20	22	18 25 0	—	—9
12 1 0	31	33				18 26 0	11	13
12 2 0	48	47				18 27 0	—	4
12 3 0	17	—18	16 0 0	59	61	18 28 0	16	18
12 4 0	58	56	16 1 0	10	—13			
12 5 0	45	40	16 2 0	50	50			
12 6 0	36	31	16 3 0	—	4	20 0 0	50	50
12 7 0	10	—8	16 4 0	51	47	20 1 0	—	1
12 8 0	53	50	16 5 0	19	—16	20 2 0	36	31
12 9 0	44	39	16 6 0	61	57	20 3 0	—	13
12 10 0	38	34	16 7 0	—	—3	20 4 0	45	48
12 11 0	—	—9	16 8 0	47	43	20 5 0	—	—3
12 12 0	45	41	16 9 0	26	—21	20 6 0	34	33
12 13 0	29	25	16 10 0	41	41	20 7 0	22	22
12 14 0	38	36	16 11 0	—	—1	20 8 0	42	43
12 15 0	17	—12	16 12 0	48	45	20 9 0	—	1
12 16 0	44	41	16 13 0	13	—15	20 10 0	30	28
12 17 0	—	9	16 14 0	38	36	20 11 0	—	9
12 18 0	40	31	16 15 0	—	1	20 12 0	34	37
12 19 0	20	—17	16 16 0	31	31	20 13 0	—	3
12 20 0	36	35	16 17 0	—	—2	20 14 0	14	19
12 21 0	—	2	16 18 0	35	36	20 15 0	—	2
12 22 0	29	26	16 19 0	—	9	20 16 0	29	28
12 23 0	19	—18	16 20 0	26	25	20 17 0	—	—8
12 24 0	28	26	16 21 0	—	4	20 18 0	13	16
12 25 0	—	—1	16 22 0	26	25	20 19 0	—	0
12 26 0	21	19	16 23 0	17	14	20 20 0	20	21
12 27 0	12	—11	16 24 0	24	25	20 21 0	—	—11
12 28 0	23	20	16 25 0	—	5	20 22 0	19	17
			16 26 0	19	19	20 23 0	—	—5
14 0 0	82	91	16 27 0	—	9	20 24 0	17	22
14 1 0	24	22	16 28 0	16	18	20 25 0	—	—7
14 2 0	61	59				20 26 0	14	17
14 3 0	9	—9	18 0 0	38	35			
14 4 0	54	50	18 1 0	27	—25	22 0 0	41	41
14 5 0	19	17	18 2 0	14	13	22 1 0	—	2
14 6 0	69	63	18 3 0	28	25	22 2 0	37	36
14 7 0	—	—2	18 4 0	35	36	22 3 0	12	—13
14 8 0	21	19	18 5 0	—	—4	22 4 0	32	29
14 9 0	25	18	18 6 0	32	32	22 5 0	—	—4
14 10 0	26	23	18 7 0	21	15	22 6 0	38	40
14 11 0	12	—10	18 8 0	42	45	22 7 0	19	—17
14 12 0	24	26	18 9 0	—	—9	22 8 0	22	22
14 13 0	18	14	18 10 0	42	39	22 9 0	—	—1
14 14 0	—	10	18 11 0	23	19	22 10 0	23	24
14 15 0	—	—7	18 12 0	50	53	22 11 0	—	—9
14 16 0	20	16	18 13 0	19	—20	22 12 0	25	23
14 17 0	—	6	18 14 0	34	34	22 13 0	—	3
14 18 0	26	26	18 15 0	—	9	22 14 0	15	17
14 19 0	—	—4	18 16 0	44	43	22 15 0	—	1
14 20 0	13	14	18 17 0	—	—12	22 16 0	—	13
14 21 0	—	7	18 18 0	33	29	22 17 0	—	7
14 22 0	27	25	18 19 0	—	1	22 18 0	20	20
14 23 0	—	—4	18 20 0	29	27	22 19 0	—	2
14 24 0	25	25	18 21 0	—	—9	22 20 0	—	12

Table 7. (Continued).

h k 0	F_o	F_c	h k 0	F_o	F_c	h k 0	F_o	F_c
22 21 0	—	8	26 21 0	—	—4	32 5 0	—	8
22 22 0	18	17	26 22 0	21	25	32 6 0	23	21
22 23 0	—	0				32 7 0	—	—3
22 24 0	20	19	28 0 0	43	45	32 8 0	24	26
22 25 0	—	4	28 1 0	—	0	32 9 0	—	6
22 26 0	15	18	28 2 0	29	31	32 10 0	23	22
			28 3 0	—	5	32 11 0	—	2
24 0 0	30	24	28 4 0	36	36	32 12 0	30	33
24 1 0	—	3	28 5 0	—	0	32 13 0	—	1
24 2 0	33	36	28 6 0	26	29	32 14 0	16	21
24 3 0	12	—13	28 7 0	—	6	32 15 0	—	0
24 4 0	14	14	28 8 0	24	24	32 16 0	22	27
24 5 0	—	0	28 9 0	—	0	32 17 0	—	4
24 6 0	45	48	28 10 0	21	17	32 18 0	17	21
24 7 0	14	—15	28 11 0	—	0			
24 8 0	20	16	28 12 0	25	22	34 0 0	21	21
24 9 0	—	0	28 13 0	—	—3	34 1 0	—	1
24 10 0	41	40	28 14 0	—	11	34 2 0	23	25
24 11 0	—	—6	28 15 0	—	—2	34 3 0	—	2
24 12 0	31	29	28 16 0	19	19	34 4 0	23	21
24 13 0	—	5	28 17 0	—	—6	34 5 0	—	3
24 14 0	33	36	28 18 0	15	16	34 6 0	23	35
24 15 0	—	—2	28 19 0	—	—2	34 7 0	—	5
24 16 0	26	24	28 20 0	15	17	34 8 0	20	20
24 17 0	—	10	28 21 0	—	—3	34 9 0	—	4
24 18 0	40	39	28 22 0	14	18	34 10 0	19	24
24 19 0	—	1				34 11 0	—	5
24 20 0	—	17	30 0 0	29	32	34 12 0	16	18
24 21 0	—	7	30 1 0	—	2	34 13 0	—	3
24 22 0	28	28	30 2 0	—	9	34 14 0	14	19
24 23 0	—	3	30 3 0	—	—3	34 15 0	—	2
24 24 0	18	17	30 4 0	23	27	34 16 0	11	16
			30 5 0	—	—3			
26 0 0	24	20	30 6 0	15	15	36 0 0	22	23
26 1 0	—	0	30 7 0	—	—5	36 1 0	—	—5
26 2 0	38	38	30 8 0	25	26	36 2 0	24	28
26 3 0	—	5	30 9 0	—	—5	36 3 0	—	1
26 4 0	25	22	30 10 0	12	11	36 4 0	20	19
26 5 0	—	9	30 11 0	—	—7	36 5 0	—	—9
26 6 0	32	33	30 12 0	27	29	36 6 0	20	27
26 7 0	—	5	30 13 0	—	—2	36 7 0	—	—1
26 8 0	21	22	30 14 0	—	10	36 8 0	11	15
26 9 0	—	8	30 15 0	—	—4	36 9 0	—	—7
26 10 0	33	32	30 16 0	21	22	36 10 0	18	21
26 11 0	—	7	30 17 0	—	0	36 11 0	—	0
26 12 0	21	19	30 18 0	11	14	36 12 0	12	14
26 13 0	—	1	30 19 0	—	2			
26 14 0	26	31	30 20 0	15	19	38 0 0	16	17
26 15 0	—	1				38 1 0	—	—4
26 16 0	20	21	32 0 0	25	23	38 2 0	10	13
26 17 0	—	—1	32 1 0	—	0	38 3 0	—	0
26 18 0	26	29	32 2 0	—	10	38 4 0	8	11
26 19 0	—	—5	32 3 0	—	—1	38 5 0	—	—7
26 20 0	17	19	32 4 0	20	21	38 6 0	23	19

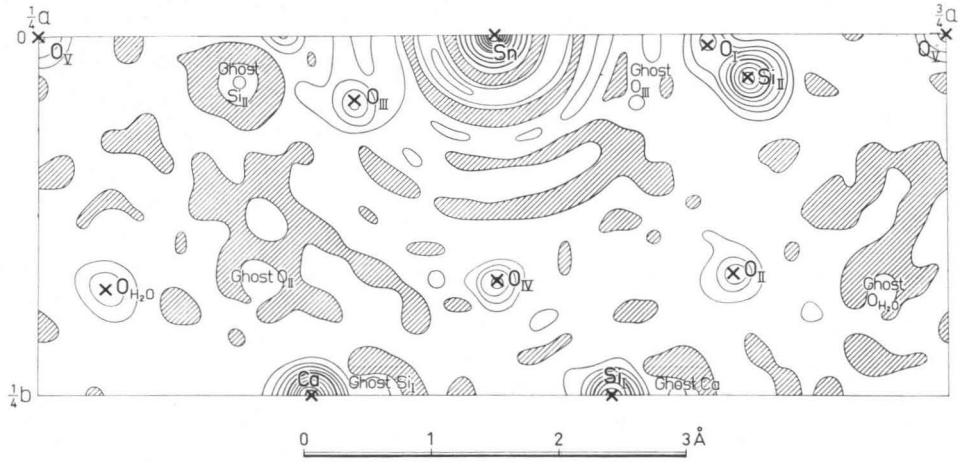

Fig. 4. Electron density projection on (001) of the asymmetric unit of stokesite. Contours at intervals of 8 *e*. Å^{-2} for Ca, Si, and O, 40 *e*. Å^{-2} for Sn (heavy lines). Negative area shaded.

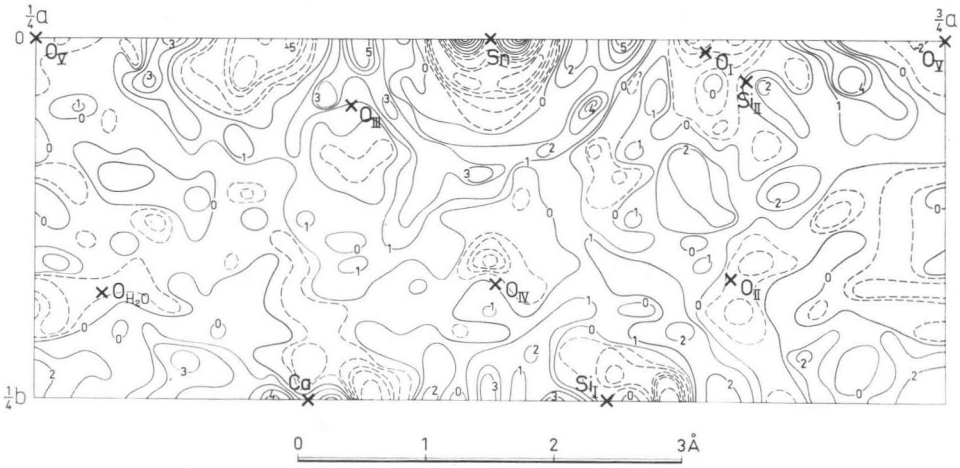

Fig. 5. Final (F_o—F_c)-synthesis of stokesite on (001). Contours at intervals of 1 *e*. Å^{-2}. Broken lines negative contours.

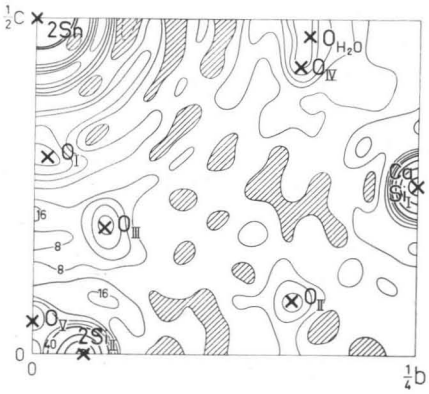

Fig. 6. Electron density projection of stokesite on (100). Contours at intervals of 8 *e*. Å^{-2}, heavy lines at intervals of 40 *e*.Å^{-2}. Negative area shaded.

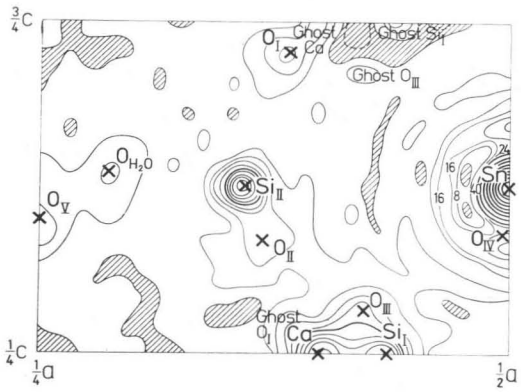

Fig. 7. Electron density projection of stokesite on (010). Contours as in Fig. 6.

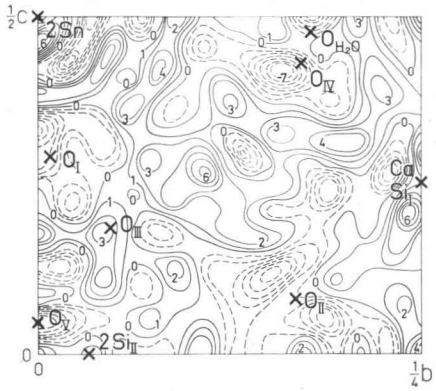

Fig. 8. Final (F_o—F_c)-synthesis of stokesite on (100). Contours at intervals of 1 *e*.Å^{-2}. Broken lines negative contours.

Fig. 9. Final (F_o—F_c)-synthesis of stokesite on (010). Contours at intervals of 2 *e*. Å^{-2}. Broken lines negative contours.

Table 8. Observed and calculated 0kl-structure factors for stokesite.

0 k l	F_o	F_c	0 k l	F_o	F_c	0 k l	F_o	F_c
0 0 0	—	370	0 17 3	49	—49	0 5 7	27	—27
0 2 0	88	91	0 19 3	38	—38	0 7 7	36	—31
0 4 0	133	171	0 21 3	39	—32	0 9 7	33	—32
0 6 0	95	114	0 23 3	32	—28	0 11 7	33	—36
0 8 0	77	76	0 25 3	22	—19	0 13 7	41	—37
0 10 0	—	12	0 27 3	14	—16	0 15 7	35	—35
0 12 0	77	80	0 29 3	13	—14	0 17 7	35	—33
0 14 0	—	—5				0 19 7	30	—30
0 16 0	48	48	0 0 4	102	128	0 21 7	26	—26
0 18 0	26	23	0 2 4	57	56	0 23 7	20	—21
0 20 0	41	36	0 4 4	104	111	0 25 7	19	—19
0 22 0	20	20	0 6 4	41	39	0 27 7	12	—16
0 24 0	48	42	0 8 4	78	75			
0 26 0	—	14	0 10 4	21	20	0 0 8	50	50
0 28 0	34	32	0 12 4	56	51	0 2 8	28	25
0 30 0	17	19	0 14 4	—	7	0 4 8	54	55
			0 16 4	40	41	0 6 8	15	15
0 1 1	50	—46	0 18 4	—	8	0 8 8	50	47
0 3 1	11	—14	0 20 4	37	33	0 10 8	16	15
0 5 1	66	—65	0 22 4	11	15	0 12 8	29	29
0 7 1	56	—56	0 24 4	33	31	0 14 8	—	9
0 9 1	56	—55	0 26 4	15	17	0 16 8	25	25
0 11 1	76	—75	0 28 4	31	30	0 18 8	—	3
0 13 1	61	—59	0 30 4	14	16	0 20 8	23	23
0 15 1	59	—54				0 22 8	—	10
0 17 1	53	—53	0 1 5	29	—31	0 24 8	22	21
0 19 1	35	—35	0 3 5	22	—26	0 26 8	14	16
0 21 1	30	—31	0 5 5	49	—47			
0 23 1	30	—28	0 7 5	50	—53			
0 25 1	16	—17	0 9 5	50	—52	0 1 9	27	—25
0 27 1	18	—17	0 11 5	67	—61	0 3 9	29	—27
0 29 1	14	—17	0 13 5	54	—55	0 5 9	25	—27
			0 15 5	46	—46	0 7 9	32	—29
0 0 2	79	89	0 17 5	38	—42	0 9 9	35	—32
0 2 2	109	107	0 19 5	37	—34	0 11 9	30	—32
0 4 2	33	26	0 21 5	25	—26	0 13 9	34	—33
0 6 2	136	136	0 23 5	21	—23	0 15 9	33	—33
0 8 2	9	10	0 25 5	18	—19	0 17 9	28	—29
0 10 2	71	70	0 27 5	16	—17	0 19 9	27	—27
0 12 2	22	22	0 29 5	12	—15	0 21 9	22	—25
0 14 2	39	37				0 23 9	17	—20
0 16 2	—	5	0 0 6	44	39			
0 18 2	42	40	0 2 6	88	93	0 0 10	32	29
0 20 2	—	2	0 4 6	40	41	0 2 10	49	49
0 22 2	37	34	0 6 6	68	61	0 4 10	28	24
0 24 2	18	17	0 8 6	22	21	0 6 10	41	40
0 26 2	30	30	0 10 6	47	49	0 8 10	16	15
0 28 2	20	20	0 12 6	—	0	0 10 10	34	29
0 30 2	30	31	0 14 6	37	36	0 12 10	—	10
			0 16 6	—	9	0 14 10	21	24
0 1 3	40	—39	0 18 6	27	27	0 16 10	—	9
0 3 3	20	—15	0 20 6	16	14	0 18 10	21	23
0 5 3	44	—41	0 22 6	29	31	0 20 10	12	12
0 7 3	37	—36	0 24 6	10	12	0 22 10	21	22
0 9 3	36	—33	0 26 6	27	29			
0 11 3	50	—52	0 28 6	15	16			
0 13 3	47	—46				0 1 11	11	—15
0 15 3	47	—45	0 1 7	23	—23	0 3 11	18	—19
			0 3 7	21	—22	0 5 11	16	—20

Table 8. (Continued).

0 k l	F_o	F_c	0 k l	F_o	F_c	0 k l	F_o	F_c
0 7 11	19	—23	0 4 12	27	28	0 5 13	13	—17
0 9 11	29	—28	0 6 12	18	16	0 7 13	15	—17
0 11 11	27	—28	0 8 12	24	22	0 9 13	17	—18
0 13 11	28	—27	0 10 12	—	8	0 11 13	18	—19
0 15 11	27	—27	0 12 12	20	21	0 13 13	17	—20
0 17 11	20	—23	0 14 12	—	6			
0 19 11	18	—20	0 16 12	14	16	0 0 14	17	19
						0 2 14	24	25
0 0 12	35	34	0 1 13	13	—16	0 4 14	16	16
0 2 12	15	15	0 3 13	16	—16	0 6 14	23	27

with the ordinary O_{IV} peak and the ghost peak for O_I is absent partly for the same cause, and partly because it has a location in the unit cell where the influence for the reflections with k odd is very small.

The negative electron density areas are shaded and it is clearly seen that these are produced mainly either by series termination ripples or by the negative depressions about the ghost peaks.

REFINEMENT OF THE PROJECTIONS ON (100) AND (010)

Space group *Pnna* projects both on (100) and (010) as two-dimensional plane group *cmm*. These two projections were refined simultaneously after the first two cycles of refinement of the (100)-projection. All the F_{0kl} are affected by tin and therefore the signs for all strong reflections are determined as soon as the tin is located. Unfortunately there are in this projection very many overlapping pairs of atoms: two Sn, Ca and Si_I, two Si_{II}, O_{IV} and O_{H_2O} (Fig. 6). Due to the two overlapping Sn atoms the diffraction ripples about them are extremely strong.

In the (010)-projection only the reflections with h and l even are influenced by tin, the other ones with h and l odd are not influenced by tin. Again the reflections affected by Sn are usually much stronger than the other ones and whilst it was possible to record 122 reflections with h and l even, only 23 with h and l odd were recorded. The formation of ghost peaks is therefore very clear in this projection also. Thus Ca, Si_I, O_I, and O_{III} atoms have very marked ghost maxima (Fig. 7). The ghost peaks for O_V and O_{H_2O} are represented by the spreading out of the peak maxima parallel to the c axis. The ghost peak of Si_{II} coincides with the actual peak and thus is not seen on the electron density map.

Six cycles of refinement of the (100)-projection and four of the (010)-projection were carried out. Four cycles were performed simultaneously.

Table 9. Observed and calculated h0l-structure factors for stokesite

h 0 l	F_o	F_c	h 0 l	F_o	F_c	h 0 l	F_o	F_c
0 0 0	—	370	34 0 2	18	25	29 0 5	—	6
2 0 0	70	113	36 0 2	32	28	31 0 5	—	—2
4 0 0	19	16	38 0 2	11	18	33 0 5	—	—7
6 0 0	46	45				35 0 5	—	—1
8 0 0	103	119	1 0 3	5	3	37 0 5	—	0
10 0 0	63	63	3 0 3	28	26			
12 0 0	51	52	5 0 3	32	29	0 0 6	44	39
14 0 0	82	91	7 0 3	—	2	2 0 6	27	25
16 0 0	59	61	9 0 3	40	—37	4 0 6	36	36
18 0 0	38	35	11 0 3	9	—9	6 0 6	57	59
20 0 0	50	50	13 0 3	8	5	8 0 6	49	44
22 0 0	41	40	15 0 3	14	10	10 0 6	20	20
24 0 0	30	25	17 0 3	12	—13	12 0 6	33	27
26 0 0	24	21	19 0 3	—	0	14 0 6	55	50
28 0 0	43	45	21 0 3	—	10	16 0 6	24	25
30 0 0	29	31	23 0 3	—	8	18 0 6	15	14
32 0 0	21	23	25 0 3	—	—7	20 0 6	24	24
34 0 0	21	21	27 0 3	—	—10	22 0 6	33	29
36 0 0	22	22	29 0 3	—	—4	24 0 6	25	25
38 0 0	16	17	31 0 3	—	4	26 0 6	27	27
			33 0 3	—	4	28 0 6	27	26
1 0 1	33	—32	35 0 3	—	2	30 0 6	9	10
3 0 1	62	—59	37 0 3	—	—3	32 0 6	—	8
5 0 1	38	—35				34 0 6	18	21
7 0 1	18	13	0 0 4	102	128			
9 0 1	32	27	2 0 4	50	55	1 0 7	12	11
11 0 1	25	23	4 0 4	26	21	3 0 7	17	15
13 0 1	5	—4	6 0 4	44	39	5 0 7	—	0
15 0 1	10	—9	8 0 4	57	58	7 0 7	—	—7
17 0 1	—	—5	10 0 4	42	40	9 0 7	—	—6
19 0 1	—	3	12 0 4	40	40	11 0 7	—	9
21 0 1	—	—6	14 0 4	57	58	13 0 7	—	—3
23 0 1	—	—9	16 0 4	37	34	15 0 7	—	—2
25 0 1	—	2	18 0 4	34	32	17 0 7	—	—9
27 0 1	—	12	20 0 4	46	46	19 0 7	—	3
29 0 1	—	5	22 0 4	33	32	21 0 7	—	6
31 0 1	—	—7	24 0 4	14	12	23 0 7	—	7
33 0 1	—	—8	26 0 4	16	16	25 0 7	—	0
35 0 1	—	1	28 0 4	37	36	27 0 7	—	—7
37 0 1	—	4	30 0 4	24	26	29 0 7	—	—6
			32 0 4	16	19	31 0 7	—	0
0 0 2	79	89	34 0 4	19	20			
2 0 2	25	22	36 0 4	16	19	0 0 8	50	50
4 0 2	86	104				2 0 8	35	33
6 0 2	121	136	1 0 5	18	—14	4 0 8	20	17
8 0 2	95	105	3 0 5	25	—23	6 0 8	36	31
10 0 2	28	25	5 0 5	10	—7	8 0 8	36	30
12 0 2	39	36	7 0 5	15	13	10 0 8	21	24
14 0 2	70	81	9 0 5	—	1	12 0 8	29	25
16 0 2	43	43	11 0 5	—	5	14 0 8	37	33
18 0 2	19	18	13 0 5	—	—7	16 0 8	17	17
20 0 2	50	46	15 0 5	—	7	18 0 8	23	22
22 0 2	51	52	17 0 5	—	0	20 0 8	37	34
24 0 2	35	37	19 0 5	—	2	22 0 8	27	27
26 0 2	25	23	21 0 5	—	—9	24 0 8	—	6
28 0 2	38	34	23 0 5	—	—8	26 0 8	9	10
30 0 2	18	19	25 0 5	—	0	28 0 8	23	24
32 0 2	15	17	27 0 5	—	9	30 0 8	20	23
						32 0 8	11	16

Table 9. (Continued).

h 0 *l*	R_o	F_c	*h* 0 *l*	F_o	F_c	*h* 0 *l*	F_o	F_c
1 0 9	—	—3	14 0 10	21	33	4 0 12	15	14
3 0 9	14	—10	16 0 10	20	23	6 0 12	19	22
5 0 9	—	—3	18 0 10	13	14	8 0 12	18	23
7 0 9	—	7	20 0 10	16	16	10 0 12	14	18
9 0 9	—	3	22 0 10	21	23	12 0 12	19	21
11 0 9	—	—1	24 0 10	14	20	14 0 12	26	28
13 0 9	—	—7	26 0 10	17	21	16 0 12	13	18
15 0 9	—	7	28 0 10	14	19	18 0 12	11	15
17 0 9	—	6				20 0 12	16	22
19 0 9	—	—1	1 0 11	—	9			
21 0 9	—	—8	3 0 11	—	9			
23 0 9	—	—4	5 0 11	—	1	1 0 13	—	—3
25 0 9	—	4	7 0 11	—	—6	3 0 13	—	—9
27 0 9	—	3	9 0 11	—	—2	5 0 13	—	0
			11 0 11	—	4	7 0 13	—	4
			13 0 11	—	—1	9 0 13	—	3
0 0 10	32	30	15 0 11	—	—2	11 0 13	—	0
2 0 10	25	22	17 0 11	—	—2			
4 0 10	17	17	19 0 11	—	3	0 0 14	17	20
6 0 10	38	37	21 0 11	—	4	2 0 14	11	17
8 0 10	38	33				4 0 14	10	16
10 0 10	18	17	0 0 12	35	34	6 0 14	21	27
12 0 10	17	16	2 0 12	23	25	8 0 14	20	25

Finally the corresponding electron density maps were calculated (Figs. 6 and 7). The reliability index for all the 173 observed F_{0kl} (Table 8) was 6.48 per cent and for the 145 observed F_{h0l} (Table 9) was 13.33 per cent. The final z coordinates of the atoms are given in Table 5.

On both projections the overlapping of atoms is conspicuous as is also the influence of series termination effect. The series termination effect is most marked for the atom O_{IV} in the projection on (010) in which the centre of the atom coincides with the first minimum about the Sn atom. In the final difference maps there are also some notable features. In (010)-projection there is a deep depression (—12 $e.Å^{-2}$) in the electron density at the position of Sn. In the corresponding F_o-synthesis the height of the peak is almost 400 $e.Å^{-2}$ and so the relative value of the depression is not very great. It may be partly due to the slightly incorrect scaling, partly incorrect temperature factor but certainly it is partly due to the inclusion in the last difference synthesis of all the strong low angle reflections which may be affected by extinction and absorption (compare Fig. 3).

It is still worth while to emphasize once more that the refinements in each projection were done omitting the most intense low angle reflections, but the final difference syntheses (Figs. 8 and 9) have been calculated using all the observed F, the only exceptions being F_{200} and F_{040}, and that, although the absolute heights of the maxima and minima in the difference

syntheses are rather great, the relative heights compared with the final electron density maps are very small. The isotropic temperature parameters used in different projections are listed in Table 6. The reliability factors R would have been slightly reduced if the temperature parameters in every projection had been treated completely separately but it did not seem necessary for the purpose of this work.

ACCURACY OF THE STRUCTURE DETERMINATION

The accuracy of the coordinates was estimated using the formula of Cruickshank (Cruickshank 1949, Ahmed and Cruickshank 1953), according to which in a well resolved projection the estimated standard deviation of an atomic coordinate, after finite series corrections, is

$$\sigma(x) = \frac{1}{A} \frac{2\pi}{a} \left\{ \sum h^2 (\Delta F)^2 \right\}^{\frac{1}{2}} \Big/ \frac{\partial^2 \varsigma}{\partial x^2}$$

where A is the area of the cell in projection and $\frac{\partial^2 \varsigma}{\partial x^2}$ the curvature of the peak at its maximum. If we take $\Delta F = |F_o - F_c|$, we get an estimate of the combined experimental and residual finite series errors.

In stokesite the (001)-projection has well resolved peaks. The (010)- and (100)-projections have a considerable amount of overlap. The z coordinates of the atoms were obtained by refining these two projections simultaneously using the x and y coordinates obtained from the (001)-projection. It is assumed that the z coordinates have been determined to about the same accuracy as the x and y coordinates, and therefore the standard deviations calculated for the x and y coordinates can be taken as standard deviations of the z coordinates.

The electron density for a number of atoms is closely approximated by the equation

$$\varsigma_r = \varsigma_o^{e^{-pr^2}} \qquad \text{(Booth 1946)}$$

The same applies closely to the projected electron density and leads to the following relation for the central curvature.

$$\left(\frac{\partial^2 \varsigma}{\partial x^2} \right)_{r=o} = -2\, p \varsigma_o$$

Table 10. Coordinates derived with three point parabola method, peak heights ς_o, $p(x)$, $p(y)$, and central curvatures $C(x)$ and $C(y)$.

Atom	x	y	ς_o $e.Å^{-3}$	$p(x)$ $Å^{-2}$	$p(y)$ $Å^{-2}$	$C(x)$ $e.Å^{-4}$	$C(y)$ $e.Å^{-4}$
Sn	0	0	379	29.4	27.6	—22 300	—20 900
Ca	.3997	¼	88	18.1	—	—3 180	—
Si_I	.0651	¼	67.0	22.7	—	—3 040	—
Si_{II}	.1406	.0312	69.3	18.3	22.0	—2 540	—3 050
O_I	.1168	.0065	26.7	20.8	14.8	—1 110	—815
O_{II}	.1309	.1680	26.8	23.9	23.2	—1 280	—1 240
O_{III}	.4244	.0485	33.9	34.5	24.0	—2 340	—1 630
O_{IV}	.0013	.1734	34.7	~30	32.5	—2 080	—2 250
O_{H_2O}	.2872	.1770	23.1	~20	~18	—920	—830
O_V	¼	0	25.3	19.8	17.1	—1 000	—860

The position of the maximum point of each peak was determined using the three point parabola method (see for example Megaw 1954). The coordinates thus derived are slightly different from those deduced from the difference synthesis. This is natural because in difference synthesis the series termination effect is eliminated as well as the influence of overlapping of atoms.

The coordinates of the atoms derived with the three point parabola method together with approximate maximum values of the electron density (ς_0) at these points are given in Table 10. The corresponding values of p and the derived central curvatures parallel to the x and y axes are also listed. As seen ς_0 varies greatly depending of course on the atom concerned but also on the position with respect to the diffraction ripples round the Sn atom. The same applies to the $p(x)$ and $p(y)$ values as well as to the $C(x)$ and $C(y)$ (central curvatures). Therefore, when calculating the standard deviations for the coordinates, the O atoms have been treated together and approximate weighted means for $C(x)$ and $C(y)$ have been taken as —1 000 $e.Å^{-4}$ and —900 $e.Å^{-4}$. Table 11 gives, according to Cruickshank's formula, estimated standard deviations. The corresponding estimated standard deviations in fractional coordinates are given in Table 5 p. 23.

The accuracy of the coordinates is fairly good. It mainly depends on the very high $\frac{\sin\Theta}{\lambda}$ value where the Fourier series were terminated. The R factors (Table 12) in this case probably give an overestimate of the accuracy of the structure. In the (100)-projection the positions of Ca, Sn, and Si_I and the y coordinate of O_V are fixed by symmetry. The R factor for this zone is 6.48 per cent. This probably reflects the accuracy of the intensity measurements. For F_{hk0} and F_{h0l} the R factors are about 10 and 14 per cent. This is still fairly good and one is prepared to say that the good agreement between

Table 11. Estimated standard deviations derived by the method of Cruickshank.

Atom	$\sigma(x)$	$\sigma(y)$	$\sigma(z)$
Sn	—	—	—
Ca	.0031 Å	—	—
Si_I	.0032 Å	—	—
Si_{II}	.0038 Å	.0034 Å	.004 Å
O	.010 Å	.011 Å	.011 Å

Note: $\sigma(z)$ not determined with the method of Cruickshank. It is, however, thought to be of the same magnitude as $\sigma(x)$ and $\sigma(y)$.

observed and calculated structure factors is completely due to the tin atom in a special position. Remembering, however, that tin does not affect every reflection it is possible to compare the R factors of reflections for which tin has and the other ones for which tin has no influence. For (001)-projection these two R factors are 9.21 and 13.92 per cent and the corresponding values for the (010)-projection are 13.54 and 11.83 respectively. This shows that the presence of tin does not improve very much the R factor directly.

The standard deviations of the interatomic distances were estimated using the formula

$$\sigma^2(l) = \{\sigma^2(x_1) + \sigma^2(x_2)\}\, cos^2\alpha + \{\sigma^2(y_1) + \sigma^2(y_2)\}\, cos^2\beta + \{\sigma^2(z_1) + \sigma^2(z_2)\}\, cos^2\gamma$$

(Ahmed and Cruickshank 1953)

where $\sigma(x_1)$, $\sigma(y_1)$ and $\sigma(z_1)$ are the standard deviations of the coordinates of the first atom, etc., and $cos\alpha$, $cos\beta$ and $cos\gamma$ are the direction cosines of the line joining the atoms.

These calculated standard deviations are given in Table 13 together with the interatomic distances. It is possible that the accuracy is slightly overestimated because of the possible influence of systematic errors caused by extinction and absorption.

The standard deviations for interatomic angles were estimated with the formula

$$\sigma^2(\Theta) = (1/lm\ sin\ \Theta)^2\, [(x_2 - x_3)^2\, \sigma^2(x_1) + (x_1 - 2x_2 + x_3)^2\, \sigma^2(x_2) + (x_2 - x_1)^2\, \sigma^2(x_3) + similar\ terms\ in\ y\ and\ z]$$

(Ahmed and Cruickshank 1953)

Table 12. The R factors for observed reflections in various projections.

	*hk*0-refinement		0*kl*-refinement		*h*0*l*-refinement		Notes
	Number of refl.	*R* (%)	Number of refl.	*R* (%)	Number of refl.	*R* (%)	
	314	9.99	173	6.48	145	13.33	For all refl.
k = even	248	9.21	—	—	—	—	Sn affects
k = odd	66	13.92	—	—	—	—	
h and l = even	—	—	—	—	122	13.54	Sn affects
h and l = odd	—	—	—	—	23	11.83	

where Θ is the bond angle, l and m the bond lengths and x_1, x_2 and x_3 the x coordinates of the three atoms concerned. The results turned out to be of the magnitude of 0.6—0.8 degrees.

DESCRIPTION OF THE STRUCTURE

From the coordinates, the most important interatomic distances with the estimated standard deviations were calculated as well as the interatomic angles; these are given in the Tables 13 and 14. Fig. 10 serves as a guide to the notation of atoms used in the tables.

Table 13. Most important interatomic distances for stokesite.

Octahedron around Sn			Octahedron around Ca		
$Sn - O_I$	(2)	2.013 ± 0.011	$Ca - O_{III}$	(2)	2.395 ± 0.011
$Sn - O_{III}$	(2)	2.054 ± 0.011	$Ca - O_{IV}$	(2)	2.403 ± 0.011
$Sn - O_{IV}$	(2)	2.033 ± 0.011	$Ca - O_{H_2O}$	(2)	2.328 ± 0.011
Average Sn — O		2.033 Å	Average Ca — O		2.376 Å
$O_I - O_{IV}$	(2)	2.917 ± 0.016	$O_{H_2O} - O_{H_2O'}$		3.315 ± 0.016
$O_I - O_{III}$	(2)	2.898 ± 0.015	$O_{H_2O} - O_{III}$	(2)	3.037 ± 0.015
$O_I - O_{IV}^*$	(2)	2.804 ± 0.015	$O_{H_2O} - O_{III'}$	(2)	3.913 ± 0.015
$O_I - O_{III}^*$	(2)	2.854 ± 0.016	$O_{H_2O} - O_{IV}$	(2)	3.106 ± 0.015
$O_{IV} - O_{III}$	(2)	2.714 ± 0.015	$O_{IV} - O_{III}$	(2)	2.714 ± 0.015
$O_{IV} - O_{III}^*$	(2)	3.057 ± 0.016	$O_{IV} - O_{III'}$	(2)	3.697 ± 0.016
			$O_{IV} - O_{IV'}$		3.814 ± 0.016
Average O — O		2.874 Å	Average O — O		3.338 Å

Tetrahedron around Si_I			Tetrahedron around Si_{II}		
$Si_I - O_{II}$	(2)	1.627 ± 0.011	$Si_{II} - O_I$		1.605 ± 0.012
$Si_I - O_{IV}$	(2)	1.599 ± 0.011	$Si_{II} - O_{II}$		1.633 ± 0.012
			$Si_{II} - O_{III}^*$		1.643 ± 0.012
			$Si_{II} - O_V$		1.631 ± 0.005
Average Si_I — O		1.613 Å	Average Si_{II} — O		1.628 Å
$O_{II} - O_{IV}$	(2)	2.626 ± 0.016	$O_I - O_{II}$		2.698 ± 0.016
$O_{II} - O_{IV'}$	(2)	2.660 ± 0.016	$O_{II} - O_{III}^*$		2.679 ± 0.016
$O_{II} - O_{II'}$		2.621 ± 0.016	$O_{III}^* - O_V$		2.672 ± 0.011
$O_{IV} - O_{IV'}$		2.611 ± 0.016	$O_I - O_{III}^*$		2.674 ± 0.015
			$O_I - O_V$		2.628 ± 0.013
			$O_V - O_{II}$		2.594 ± 0.011
Average O — O		2.634 Å	Average O — O		2.657 Å

Table 14. Most important interatomic angles for stokesite.

Octahedron around Sn		Octahedron around Ca	
O_I — Sn — O_{I^*}	180°	O_{IV} — Ca — $O_{H_2O'}$	172°32′
O_{III} — Sn — O_{III^*}	180°	$O_{IV'}$ — Ca — O_{H_2O}	172°32′
O_{IV} — Sn — O_{IV^*}	180°	O_{III} — Ca — $O_{III'}$	163°46′
O_I — Sn — O_{III}	90°53′	O_{IV} — Ca — $O_{VI'}$	105°05′
O_{I^*} — Sn — O_{III^*}	90°53′	O_{IV} — Ca — O_{III}	68°53′
O_I — Sn — O_{III^*}	89°07′	$O_{IV'}$ — Ca — $O_{III'}$	68°53′
O_{I^*} — Sn — O_{III}	89°07′	O_{IV} — Ca — O_{H_2O}	82°05′
O_I — Sn — O_{IV}	92°16′	$O_{IV'}$ — Ca — $O_{H_2O'}$	82°05′
O_{I^*} — Sn — O_{IV^*}	92°16′	O_{IV} — Ca — $O_{III'}$	100°49′
O_I — Sn — O_{IV^*}	87°44′	$O_{IV'}$ — Ca — O_{III}	100°49′
O_{I^*} — Sn — O_{IV}	87°44′	O_{III} — Ca — O_{H_2O}	80°00′
O_{III} — Sn — O_{IV}	83°00′	$O_{III'}$ — Ca — $O_{H_2O'}$	80°00′
O_{III^*} — Sn — O_{IV^*}	83°00′	O_{III} — Ca — $O_{H_2O'}$	111°53′
O_{III} — Sn — O_{IV^*}	97°00′	$O_{III'}$ — Ca — O_{H_2O}	111°53′
O_{III^*} — Sn — O_{IV}	97°00′	O_{H_2O} — Ca — $O_{H_2O'}$	90°48′

Tetrahedron around Si_I		Tetrahedron around Si_{II}	
O_{II} — Si_I — O_{IV}	108°57′	O_I — Si_{II} — O_{II}	112°53′
$O_{II'}$ — Si_I — $O_{IV'}$	108°57′	O_I — Si_{II} — O_{III}	110°54′
O_{II} — Si_I — $O_{IV'}$	111°05′	O_I — Si_{II} — O_V	108°37′
$O_{II'}$ — Si_I — O_{IV}	111°05′	O_{II} — Si_{II} — O_{III}	109°43′
O_{II} — Si_I — $O_{II'}$	107°18′	O_{II} — Si_{II} — O_V	105°11′
O_{IV} — Si_I — $O_{VI'}$	109°30′	O_{III} — Si_{II} — O_V	109°02′
Average O — Si_I — O	109°29′	Average O — Si_{II} — O	109°23′

Si_{II} — O_{II} — Si_I	139°57′
Si_{II} — O_V — Si_{II^*}	162°26′

In Figs. 11, 12, and 13 the silicate framework of stokesite is schematically represented. In Fig. 11 it is seen that the structure represents a peculiar type of chain silicate the chains being parallel to the *b* axes. There are six tetrahedra in a repeat unit of tetrahedral structure. The chains are a helical like arrangement about the screw diads. In Fig. 12 the $(SiO_3)_n$ chains are projected into the plane perpendicular to the *b* axes and the screw diads. As seen the spiral-like structure is far from complete but has been strongly deformed. Fig. 13 shows the chains viewed along the *a* axis.

The Si—O—Si angles are 139°57′ and 162°26′ (Table 14). In a statistical treatise on Si—O—Si angles in different kinds of silicate structures, Liebau (1961) gives 140° as a mean value for this angle (the smallest angle he used for this mean was 129° and the greatest 166°). The Si—O—Si angles in stokesite are thus in accordance with the results of Liebau.

In a review of the measured Si—O and Al—O distances (in tetrahedral coordination) Smith (1954) comes to the conclusion that Si—O = 1.60 ± 0.01

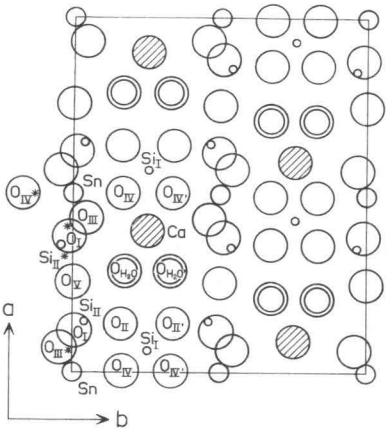

Fig. 10. Schematical representation of the projection on (001) of the unit cell content of stokesite.

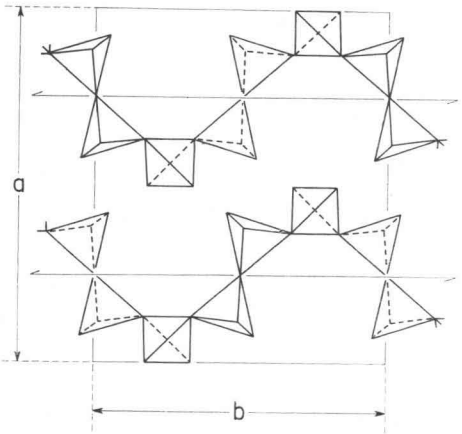

Fig. 11. $(SiO_3)_n$ framework of stokesite viewed along the *c* axis.

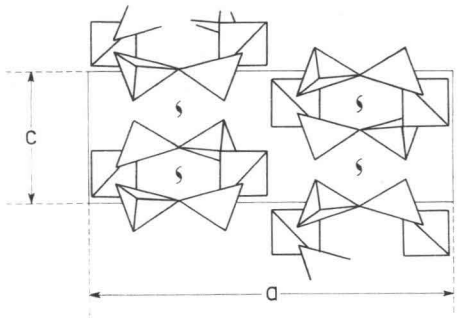

Fig. 12. $(SiO_3)_n$ framework of stokesite viewed along the *b* axis.

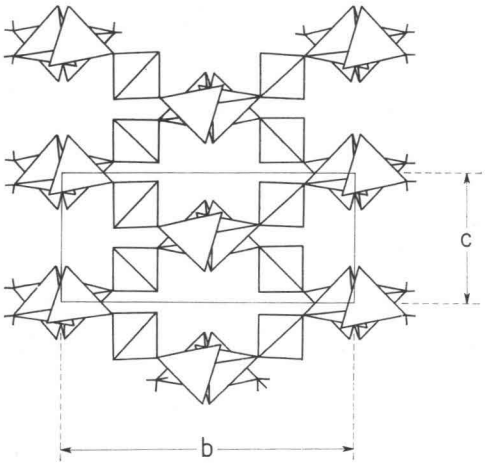

Fig. 13. $(SiO_3)_n$ framework of stokesite viewed along the *a* axis.

Å and Al—O = 1.78 ± 0.02 Å [1]). In the case of stokesite there is no question of Al substitution because all the tetrahedral sites are occupied by Si. As seen in Table 13 the mean value for the distance Si_I—O is 1.613 Å and Si_{II}—O 1.628 Å thus confirming the accuracy of the structure determination. Comparison of the interatomic distances within the coordination polyhedron $[Si_IO_4]$ and within the $[Si_{II}O_4]$ tetrahedron shows that the tetrahedra are only very slightly deformed.

When applying Cruickshank's significance test (Lipson and Cochran 1957, p. 309) to the bond length differences in the $[Si_IO_4]$ tetrahedron it is seen that the bond length variation 1.627—1.599 is possibly significant. The bond length differences in the $[Si_{II}O_4]$ tetrahedra are not significant, the only exception being the bond Si_{II}—O_I which may be significantly shorter than the others. Significance tests applied to the O—O distances within the tetrahedra show that some of the O—O distances in the $[Si_IO_4]$ tetrahedra are possibly significantly different whilst some of the O—O distances in the $[Si_{II}O_4]$ tetrahedra are significantly different.

An examination of Figs. 11—13 showing the silicate framework structure makes it clear that there are »tunnels» parallel to the *c* axis as well as parallel to the *a* axis. The former are occupied by Ca ions and water molecules, the latter by Sn ions.

Ca is coordinated by six oxygen atoms: $O_{,IV}$ $O_{IV'}$ (adjacent chain), O_{III}, $O_{III'}$, O_{H_2O}, and $O_{H_2O'}$. The coordination number six is rare for Ca. Some of the other known silicate structures containing octahedral groups $[CaO_6]$ are monticellite (Eitel 1954, p. 20), foshagite (Gard and Taylor 1960), xonotlite (Heller and Taylor 1956, pp. 46—47), and possibly some other calcium silicates. Usually Ca has a higher coordination with oxygen (7 or 8). Lower coordination numbers are probably more stable at higher temperatures. The oxygen atoms O_{IV}, $O_{IV'}$, and O_{III} ($O_{III'}$) belong to three different $(SiO_3)_n$ chains, Ca ions therefore hold the corresponding chains together. The coordination octahedron is rather irregular as is clearly seen from the interatomic lengths and angles (Tables 13 and 14). Ca—O distances vary from 2.33 to 2.40 Å (this variation is significant according to Cruickshank's significance test) the shortest distance being Ca—O_{H_2O} as is natural because all the other oxygen atoms belong at the same time to the $(SiO_3)_n$ chains and, due to the vicinity of Si^{4+}, the Ca^{2+} has »migrated» slightly towards O_{H_2O}. O—O distances in the octahedron vary from 2.71 to 3.81 Å.

Sn is coordinated more regularly than Ca in octahedral groups $[SnO_6]$. The Sn—O distances vary very little (the difference between bond lengths Sn—O_I and Sn—O_{III}, however, is significant) being of the magnitude

[1]) Smith and Bailey (1962): The average of all Si—O distances in a structure depends on the extent of the tetrahedral linkage, changing from 1.61 Å in tectosilicates to 1.63 Å in nesosilicates (Program, 1962 Annual Meetings, The Geological Society of America, etc.)

2.03 Å which corresponds to the usual distance, 2.054 ± 0.014 Å, between Sn^{4+} and O (International Tables for X-ray Crystallography, Vol. III, p. 264). For Sn^{2+} the corresponding distance is 2.21 Å (coordination number 4). The oxygen to oxygen distances in the octahedron vary from 2.71 to 3.06 Å showing much more regularity than in the coordination group $[CaO_6]$. The oxygen atoms forming the $[SnO_6]$ group belong to four different $(SiO_3)_n$ chains. Thus Sn binds these chains together.

In the summary of previous work on stokesite the results on water loss at different temperatures were given (p. 10). These indicate that the water molecules are rather strongly bound to the structure. The sharp peaks on the electron density maps also show that the water molecules have fixed positions. It is probable that the adjacent Ca ion causes the water molecules to be polarized and that hydrogen bonds occur between O_{H_2O} and some of the oxygen atoms belonging to the silicate framework and possibly $O_{H_2O'}$. Due to the uncertainty in the coordinates of water molecules [1]) it is difficult to determine which of the interatomic distances really represent the hydrogen bonds; small shifts of the water molecules could change the situation completely.

Pauling's valence rule (e. g., Pauling 1954) is also approximately fulfilled. If it were possible to decide which of the interatomic distances corresponded to hydrogen bonds then it is probable that the rule would be completely fulfilled.

The structure given here for stokesite can also explain perfectly the observed cleavages. Thus both good cleavage directions are such that the silicate chains are preserved when cleaved.

---

[1]) E.s.d. were determined as a mean for all oxygen atoms from the (001)-projection. The central curvatures for water molecules were considerable less than this mean value. In the other two projections the water molecules are either superposed by O_{IV} or the maxima in electron density is elongated parallel to the *c* axis. Thus the e.s.d. derived from the (001)-projection and applied also to the *z* coordinates are not at all reliable in the case of water molecules.

CORRELATION OF THE STRUCTURE TO OTHER KNOWN CHAIN SILICATE STRUCTURES

In the following we shall not consider the classification of the silicate structures as a whole but our attention is directed only to one special group of the chain silicates. The chain structures are generally divided into the following subtypes: single chains, double chains, multiple chains and possibly mixed chains (Liebau 1959, 1960, 1961; Zoltai 1960). In the following

Table 15. Classification of chain silicates with single chains.

Number of tetrahedra in a repeat unit	Examples	References
1	Not yet found	
2	Pyroxenes	Warren and Bragg 1928
	Carpholite-ferrocarpholite $MnAl_2(OH)_4Si_2O_6$ — $FeAl_2(OH)_4Si_2O_6$	MacGillavry, Korst, Moore, and Plas 1956, Strunz 1957.
	Ramsayite (Lorenzenite) $Na_2Ti_2O_3Si_2O_6$	Schurtz 1955
	Li_2SiO_3	Seeman 1956
	$BaSiO_3$(h)	Liebau 1960
3	β-wollastonite $CaSiO_3$	Dornberger-Schiff, Liebau, and Thilo 1955
	Bustamite $CaMn(SiO_3)_2$	Liebau 1960
	β-$MnSiO_3$	Liebau 1960
	Pectolite $Ca_2NaHSi_3O_9$	Buerger 1956
	Schizolite $(Ca,Mn)_2NaHSi_3O_9$	Liebau 1957
	Foshagite $Ca_4Si_3O_9(OH)_2$	Gard and Taylor 1960
4	Not yet found [1])	
5	Rhodonite $(Mn,Ca)SiO_3$	Liebau, Hilmer, and Lindeman 1959
6	Stokesite $CaSnSi_3O_9 \cdot 2H_2O$	The present paper
7	Pyroxmangite $(Mn,Fe,Ca,Mg)SiO_3$	Liebau 1959

[1]) According to an oral communication from Dr. F. Liebau, however, the single chain structure with four tetrahedra in a repeat unit is represented by an as yet unpublished silicate structure.

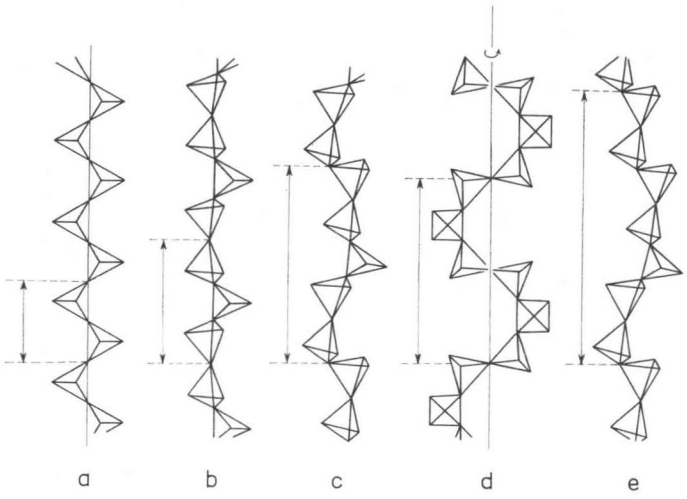

Fig. 14. Schematical representation of the single chain types found in silicates.

treatment we are only interested in the single chain structures to which stokesite also belongs. Liebau (1959, 1961) classifies these conveniently on the basis of the number of tetrahedra in a repeat unit of tetrahedral structure and this classification for chain silicates seems to be commonly accepted (Zoltai 1960, Wells 1962, p. 792). Accordingly it is possible to group the known single chain silicates as given in Table 15.

In Fig. 14 there is a schematic representation of all the known single chain silicate structure types. (a) represents the case of pyroxenes etc, (b) β-wollastonite etc, (c) rhodonite, (d) stokesite, and (e) pyroxmangite. Stokesite is the first silicate having six tetrahedra in a repeat unit. As seen, its silicate framework does not resemble any other chain silicate type. Liebau (1959) emphasized that the chains of β-wollastonite, rhodonite, and pyroxmangite resemble each other very much. The »three tetrahedra unit» of β-wollastonite is a part of the »five tetrahedra unit» in rhodonite which correspondingly is part of the »seven tetrahedra unit» in pyroxmangite. The two other known silicate chains do not resemble this scheme at all.

The single chain with one tetrahedron in a repeat unit has not been found in silicates. It has been found, however, in other inorganic compounds as in $(NH_4)_2CuCl_3$, $(NH_4)_2CuBr_3$, and K_2CuCl_3 (Brink and MacGillavry 1949, Brink and van Argel 1952), $CuGeO_4$ (Ginetti 1954). The single chain with four tetrahedra in a repeat unit is the one other which has not yet been found in silicates. It is, however, also found in the inorganic compounds $(AgPO_3)_n$ and $(NaPO_3)_n$ (Jost 1961). Similar chains to those found in pyroxenes have

been found in very many compounds in addition to silicates. For example some germanates (Roth 1955), phosphates (Corbridge 1956), arsenates (Hilmer and Dornberger-Schiff 1956), vanadates (Liebau 1959), and fluoberyllates (Hahn 1953) have this kind of chain structure. The chain structure similar to that in β-wollastonite is also present in some germanates and fluoberyllates (Liebau 1957). It seems evident that no structure with repeat unit of six tetrahedra has been reported before the present work. The chains in stokesite bear some resemblance to the chains in $(AgPO_3)_n$ in that in both structures the chains are spiral-like. This is, however, the only resemblance; the latter has only four tetrahedra in a repeat unit.

REFERENCES

AHMED, F. R. and CRUICKSHANK, D. W. J. (1953) A refinement of the crystal structure analysis of oxalic acid dihydrate. Acta Cryst. 6: 385—392.

BOOTH, A. D. (1946) The accuracy of atomic coordinates derived from Fourier series in X-ray structure analysis. Proc. Roy. Soc. (London) (A) 188: 77—79.

BRINK, CLARA and MACGILLAVRY, C. H. (1949) The crystal structure of K_2CuCl_3 and isomorphous substances. Acta Cryst. 2: 158—163.

—»— and VAN ARGEL, A. E. (1952) The crystal structures of $(NH_4)_2CuCl_3$ and $(NH_4)_2CuBr_3$. Acta Cryst. 5: 506—510.

BUERGER, M. J. (1949) X-ray crystallography. New York.

—»— (1956) The determination of the crystal structure of pectolite, $Ca_2NaHSi_3O_9$. Z. Kristallogr. 108: 248—262.

—»— (1960) Crystal-structure analysis. New York.

ČECH, F. (1961) Occurrence of stokesite in Czechoslovakia. Mineral. Mag., 32: 673—675.

COCHRAN, W. (1948) The correction of X-ray intensities for polarization and Lorenz factors. J. Scientific Instruments 25: 253—254.

—»— (1951) Some properties of the $(F_o—F_c)$-synthesis. Acta Cryst. 4: 408—411.

CORBRIDGE, D. E. C. (1956) The crystal structure of rubidium metaphosphate. Acta Cryst. 9: 308—314.

CRUICKSHANK, C. W. J. (1949) The accuracy of electron-density maps in X-ray analysis with special reference to dibenzyl. Acta Cryst. 2: 65—82.

DORNBERGER-SCHIFF, K., LIEBAU, F. and THILO, E. (1955) Zur Struktur des β-Wollastonits, des Maddrelleschen Salzes und des Natriumpolyarsenats. Acta Cryst. 8. 752—754.

EITEL, WILHELM (1954) The physical chemistry of the silicates. Chicago.

EVANS, JR. H. T. and EKSTEIN, MIRIAM G. (1952) Tables of absorption factors for spherical crystals. Acta Cryst. 5: 540—542.

FORSYTH, J. B. and WELLS, M. (1959) On an analytic approximation to the atomic scattering factor. Acta Cryst. 12: 412—415.

GARD, J. A. and TAYLOR, H. F. W. (1960) The crystal structure of foshagite. Acta Cryst. 13: 785—793.

GAY, P. and RICKSON, K. O. (1960) X-ray data on stokesite. Mineral Mag. 32: 433—435.

GINETTI, Y. (1954) Structure cristalline du métagermanate de cuivre. Bull. Soc. Chim. Belgique 63: 209—216.

HAHN, THEO (1953) Modellbeziehungen zwischen Silikaten und Fluoberyllaten. Neues Jb. Miner., Abh. 86: 1—65.

HELLER, L. and TAYLOR, H. F. W. (1956) Crystallographical data for the calcium silicates. London.

HENRY, NORMAN F. M. and LONSDALE, KATHLEEN (1952) International tables for X-ray crystallography. Vol. I. Symmetry groups. Birmingham.

Hilmer, Waltrand and Dornberger-Schiff, Käte (1956) Die Kristalstruktur von Lithiumpolyarsenat $(LiAsO_3)_x$. Acta Cryst. 9: 87—88.

Hutchinson, A. (1900) On stokesite, a new mineral containing tin, from Cornwall. Mineral. Mag. 12: 274—281.

Jost, K. H. (1961) Die Struktur des Silberpolyphosphats $(AgPO_3)_x$. Acta Cryst. 14: 779—784.

—»— (1961) Die Struktur des Kurrol'schen Na-Salzes $(NaPO_3)_x$. Typ A. Acta Cryst. 14: 844—847.

Liebau, Friedrich (1957) Über die Struktur des Schizoliths. Neues Jb. Miner., Mh. 1957: 227—229.

—»— (1957) On the crystal chemistry of silicates, germanates, arsenates, vanadates and alkalifluoberyllates. Acta Cryst. 10: 790—791.

—»— (1959) Über die Kristallstruktur des Pyroxmangits (Mn,Fe,Ca,Mg)SiO_3. Acta Cryst. 12: 177—181.

—»— (1960) Zur Kristallchemie der Silikate, Germanate und Fluoberyllate des Formeltypus ABX_3. Neues Jahrb. Miner., Abh. 94: 1 209—1 222.

—»— (1961) Ein erweitertes System der Silikate. Fortschr. Mineral. 39: 38—39.

—»— (1961) Untersuchungen über die Grösse des Si—O—Si Valenzwinkels. Acta Cryst. 14: 1 103—1 109.

—»— Hilmer, Waltrand and Lindemann, Gerhard (1959) Über die Kristallstruktur des Rhodonits. (Mn, Ca)SiO_3. Acta Cryst. 12: 182—187.

Lipson, H. and Cochran, W. (1957) The determination of crystal structures. The crystalline state. Vol. III. London.

MacGillavry, C. H., Korst, W. L., Moore, E. J. W. and van der Plas, H. J. (1956) The crystal structure of ferrocarpholite. Acta Cryst. 9: 773—776.

—»— and Rieck, Gerald D. (1962) International tables for X-ray crystallography. Vol. III. Physical and chemical tables. Birmingham.

Megaw, Helen D. (1954) Location of atomic centres in an electron density synthesis. Acta Cryst. 7: 771.

Pauling, Linus (1954) The nature of the chemical bond. New York.

Roth, Robert S. (1955) Synthetic alkaline earth germanates isostructural with enstatite and pseudowollastonite. Amer. Mineralogist 40: 332.

Seeman, H. (1956) Die Kristallostruktur des Lithiummetasilikates, $(Li_2SiO_3)_x$. Acta Cryst. 9: 251—252.

Shurtz, Robert F. (1955) Lorenzenite $Na_2Ti_2O_3Si_2O_6$. Amer. Mineralogist 40: 335.

Smith, J. V. (1954) A review of the Al—O and Si—O distances. Acta Cryst. 7: 479—481.

Strunz, H. (1957) Ferrokarpholith-Karpholith. Acta Cryst. 10: 238.

Warren, B. and Bragg, W. Lawrence (1928) The structure of diopside, $CaMg(SiO_3)_2$. Z. Kristallogr. 69: 168—193.

Wells, A. F. (1962) Structural inorganic chemistry. Oxford.

Wilson, A. J. C. (1942) Determination of absolute from relative X-ray intensity data. Nature 150: 152.

Zoltai, Tibor (1960) Classification of silicates and other minerals with tetrahedral structures. Amer. Mineralogist 45: 960—973.